

Synthesis and characterizations of boron and nitrogen co-doped high pressure and high temperature large single-crystal diamonds with increased mobility

Xin-Yuan Miao(苗辛原), Hong-An Ma(马红安), Zhuang-Fei Zhang(张壮飞), Liang-Chao Chen(陈良超), Li-Juan Zhou(周丽娟), Min-Si Li(李敏斯), and Xiao-Peng Jia(贾晓鹏)

Citation: Chin. Phys. B, 2021, 30 (**6**): 068102. DOI: 10.1088/1674-1056/abf12c
Journal homepage: http://cpb.iphy.ac.cn; http://iopscience.iop.org/cpb

What follows is a list of articles you may be interested in

Characteristics of urea under high pressure and high temperature

Shuai Fang(房帅), Hong-An Ma(马红安), Long-Suo Guo(郭龙锁), Liang-Chao Chen(陈良超), Yao Wang(王遥), Lu-Yao Ding(丁路遥), Zheng-Hao Cai(蔡正浩), Jian Wang(王健), Xiao-Peng Jia(贾晓鹏)

Chin. Phys. B, 2019, 28 (**9**): 098101. DOI: 10.1088/1674-1056/ab3445

Different effect of NiMnCo or FeNiCo on the growth of type-IIa large diamonds with Ti/Cu as nitrogen getter

Shang-Sheng Li(李尚升), He Zhang(张贺), Tai-Chao Su(宿太超), Qiang Hu(胡强), Mei-Hua Hu(胡美华), Chun-Sheng Gong(龚春生), Hon-An Ma(马红安), Xiao-Peng Jia(贾晓鹏), Yong Li(李勇)

Chin. Phys. B, 2017, 26 (**6**): 068102. DOI: 10.1088/1674-1056/26/6/068102

Synthesis of N-type semiconductor diamonds with sulfur, boron co-doping in FeNiMnCo-C system at high pressure and high temperature

He Zhang(张贺), Shangsheng Li(李尚升), Taichao Su(宿太超), Meihua Hu(胡美华), Hongan Ma(马红安), Xiaopeng Jia(贾晓鹏), Yong Li(李勇)

Chin. Phys. B, 2017, 26 (**5**): 058102. DOI: 10.1088/1674-1056/26/5/058102

Effects of catalyst height on diamond crystal morphology under high pressure and high temperature

Ya-Dong Li(李亚东), Xiao-Peng Jia(贾晓鹏), Bing-Min Yan(颜丙敏), Ning Chen(陈宁), Chao Fang(房超), Yong Li(李勇), Hong-An Ma(马红安)

Chin. Phys. B, 2016, 25 (**4**): 048103. DOI: 10.1088/1674-1056/25/4/048103

Controllable synthesis of fullerene nano/microcrystals and their structural transformation induced by high pressure

Yao Ming-Guang, Du Ming-Run, Liu Bing-Bing

Chin. Phys. B, 2013, 22 (**9**): 098109. DOI: 10.1088/1674-1056/22/09/098109

Synthesis and characterizations of boron and nitrogen co-doped high pressure and high temperature large single-crystal diamonds with increased mobility*

Xin-Yuan Miao(苗辛原)[1,†], Hong-An Ma(马红安)[2], Zhuang-Fei Zhang(张壮飞)[3], Liang-Chao Chen(陈良超)[3], Li-Juan Zhou(周丽娟)[1], Min-Si Li(李敏斯)[1], and Xiao-Peng Jia(贾晓鹏)[2]

[1] *College of Physics, Guangxi University of Science and Technology, Liuzhou* 545006, *China*

[2] *State Key Laboratory of Superhard Materials, College of Physics, Jilin University, Changchun* 130012, *China*

[3] *Key Laboratory of Material Physics of Ministry of Education, and School of Physical Engineering, Zhengzhou University, Zhengzhou* 450052, *China*

(Received 23 January 2021; revised manuscript received 19 March 2021; accepted manuscript online 24 March 2021)

We synthesized and investigated the boron-doped and boron/nitrogen co-doped large single-crystal diamonds grown under high pressure and high temperature (HPHT) conditions (5.9 GPa and 1290 °C). The optical and electrical properties and surface characterization of the synthetic diamonds were observed and studied. Incorporation of nitrogen significantly changed the growth trace on surface of boron-containing diamonds. X-ray photoelectron spectroscopy (XPS) measurements showed good evident that nitrogen atoms successfully incorporate into the boron-rich diamond lattice and bond with carbon atoms. Raman spectra showed differences on the as-grown surfaces and interior between boron-doped and boron/nitrogen co-doped diamonds. Fourier transform infrared spectroscopy (FTIR) measurements indicated that the nitrogen incorporation significantly decreases the boron acceptor concentration in diamonds. Hall measurements at room temperature showed that the carriers concentration of the co-doped diamonds decreases, and the mobility increases obviously . The highest hole mobility of sample BNDD-1 reached 980 $cm^2 \cdot V^{-1} \cdot s^{-1}$, possible reasons were discussed in the paper.

Keywords: high pressure and high temperature (HPHT), diamond, growth of crystal, boron and nitrogen co-doped diamond

PACS: 81.10.Fq, 61.72.S–, 64.70.dg, 07.57.Ty **DOI:** 10.1088/1674-1056/abf12c

1. Introduction

Nitrogen and boron are the most familiar impurities in synthesized diamonds by high pressure and high temperature (HPHT). As a shallow energy level acceptor, boron impurity in diamond has an ionization energy of 0.37 eV and can be activated at room temperature.[1] So boron-doped diamond (BDD) is considered as a promising p-type semiconductor material, which has many outstanding properties such as high hardness, high thermal conductivity, and high mobility.[2–4] As the boron concentration in BDD increases, the acceptor ionization energy decreases because the acceptor energy levels increase and merge into energy band. The BDD films present a metal–insulator transition for a boron concentration on the order of 4.5×10^{20} cm^{-3}.[5] Superconductivity in diamond can even be observed in some heavily boron-doped diamond films and growth surface of heavily HPHT single-crystal diamonds when the boron concentration increases to the order of 10^{21} cm^{-3}.[6,7] However, the boron concentration threshold is not often reached because of the compensating nitrogen donors.[8] In BDD with boron concentration below the threshold of metal–insulator transition, just only a small part (about 1%–2%) of total boron atoms can be ionized.[8] As the investigation of Pernot, the low carrier mobility in BDD with high boron concentration (below the threshold of metal–insulator transition) is attributed to the scattering mechanism caused by the dominant neutral boron acceptors, i.e., neutral impurity (ni).[9] And the ni mode could be the main factor limiting the mobility and conductivity in BDD.

Nitrogen has a very high solubility in diamond and it enters the diamond lattice as a substitutional impurity in the process of crystal growth both by HPHT and CVD.[10–12] As a typical deep donor in diamond, nitrogen impurity can hardly be ionized at room temperature, but can easily compensate boron acceptors and decrease the concentration of neutral boron impurity.[8,13] The nitrogen and boron co-doping of CVD diamond films and HPHT diamonds has been studied by some groups. The improvements on electron field emission properties and mechanical properties, and some variations of optical characterization were also observed in previous reports.[14–17] Nevertheless, the reports concentrated on the nitrogen and boron co-doping of HPHT large single-crystal diamonds are scarce. There are only a few relevant reports in which the diamonds present very poor electrical property due to the low boron concentration.[14,17,18] In this paper, boron-

*Project supported by the National Natural Science Foundation of China (Grant Nos. 51772120, 11704340, 11604246, and 11865005), the Scientific and Technological Project in Henan Province, China (Grant No. 202102210198), the Natural Science Foundation of Guangxi (China) (Grant No. 2018GXNSFAA281024), and Doctor Start-up Foundation of Guangxi University of Science and Technology (Grant No. 20Z38).

†Corresponding author. E-mail: miaoxy@gxust.edu.cn

© 2021 Chinese Physical Society and IOP Publishing Ltd

doped single-crystal diamonds (BDD) and boron/nitrogen co-doped single-crystal diamonds (BNDD) with low resistivity and increased mobility were synthesized by HPHT, and the effects of nitrogen incorporation on optical and electrical properties of BDD and BNDD were investigated.

2. Experimental details

The synthetic diamonds in this study were grown on a {111} face of seed by the temperature gradient growth (TGG) method in Fe–Ni–C–B environments under 5.9 GPa and 1290 °C using a China-type large-volume cubic high pressure apparatus (CHPA) (SPD-6 ×1200). A schematic diagram of the cell assembly used for crystal growth is shown in Fig. 1(a).

High-purity graphite was used as the carbon source and high-purity amorphous boron powder was used as the boron source. Ti was used as the nitrogen getter in the growth system to synthesize BDD. NaN_3 powder was used as the nitrogen source to synthesize BNDD. We grew the diamonds with different boron and nitrogen concentrations by means of changing the corresponding additive contents (weight ratio to carbon source) in the original growth systems. The specific information of doping is listed in Table 1. The as-grown diamonds presented octahedral habitus and were cut into the {111} square plates with a thickness of about 0.4 mm by laser. The plates were polished and cleaned by the boiling concentrated sulfuric acid and alcohol successively before characterization. The {111} surface of the as-grown samples were observed by scanning electron microscope (SEM). The plate samples were characterized by x-ray photoelectron spectroscopy (XPS), Fourier transform infrared spectroscopy (FTIR), and Raman spectroscopy. The Hall effect of the plates samples was measured using the van der Pauw four-probe method at room temperature, and Ag was used as the electrode.

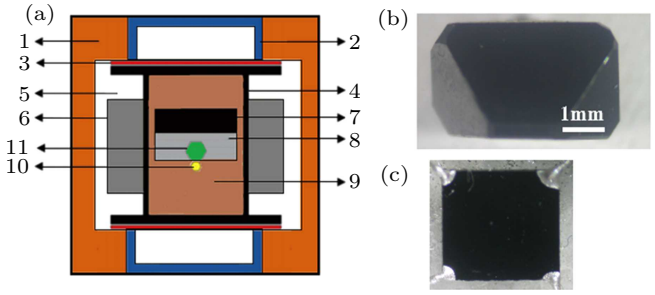


Fig. 1. (a) Assembly of high-pressure chamber: 1. pyrophyllite; 2. conductive rim; 3. cooper sheet; 4. graphite; 5. dolomite; 6. thermal insulation material; 7. carbon source; 8. catalyst alloy; 9. insulating material; 10. seed; 11. as-grown crystal. (b) As-grown diamond of BDD-1. (c) {111} square plate sample BDD-1.

3. Results and discussion

All the grown crystals are opaquely black octahedral diamonds. In order to observe the effect of nitrogen on the surface morphology of boron-doped diamonds, the {111} surfaces of original samples BDD-2 and BNDD-2 were characterized by SEM. As shown in Fig. 2, the growth surfaces of two diamonds are not smooth. There are a lot of triangular step growth defects with different sizes on the {111} surface of boron-doped samples BDD-2 and all the triangular defects have the regular orientation and uniform angle of 60° consistent with angles of the {111} surface. The orientation should be the direction of carbon atoms stacking in the growth layer. As incorporation of nitrogen, the surface morphology of BNDD-2 is distinctive. The crystal surfaces, not only {111} surface, are covered with obviously dentritic defects and no triangular step defects are observed. We consider that such dentritic defects could not be growth traces of crystals, but generated in process of condensing of molten metallic catalyst while the diamonds no longer grow. The dentritic defects were also observed in nitrogen and boron co-doped diamonds grown in a system with h-BN additive in previous report.[14] It could be relevant to abundant nitrogen and boron impurities in the growth system.

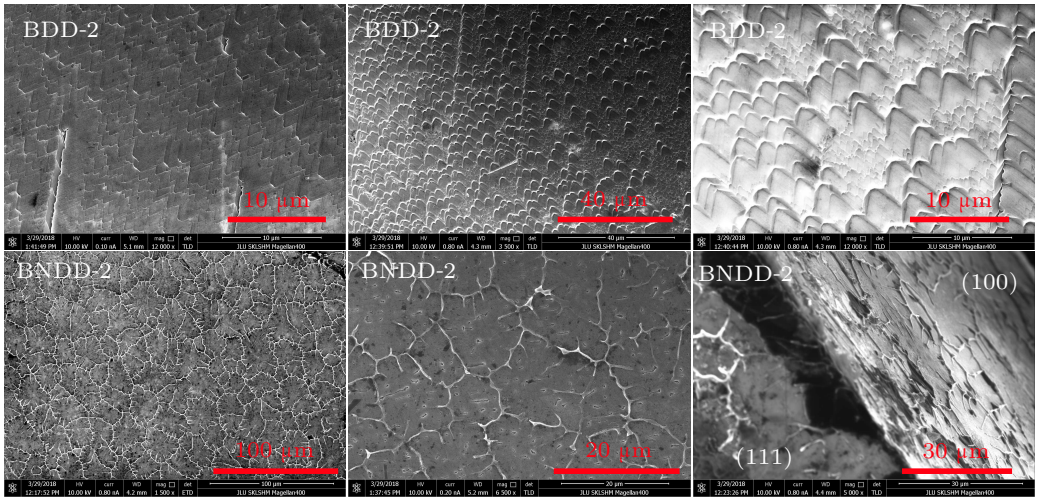


Fig. 2. SEM images of {111} growth surfaces of samples BDD-2 and BNDD-2.

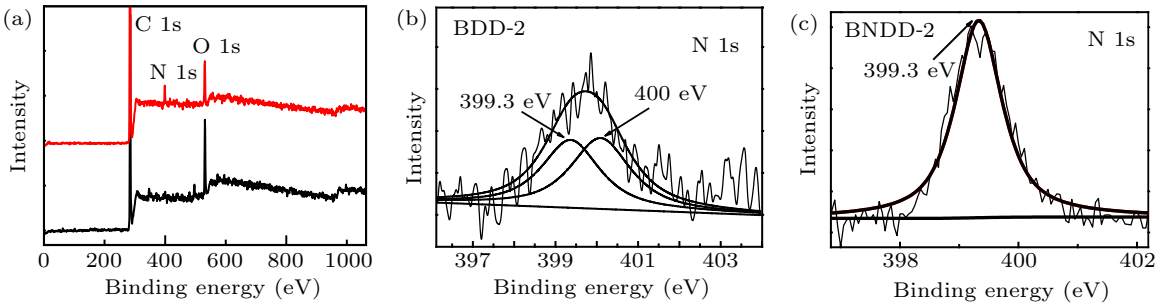


Fig. 3. (a) XPS spectra of boron doped diamond (BDD-2) and boron/nitrogen co-doped diamond (BNDD-2). The two spectra are the amplification of N 1s peaks of (b) BDD-2 and (c) BNDD-2.

In such boron-rich large single-crystal diamonds, nitrogen hardly can be tested by regular FTIR methods. In order to study the states of nitrogen impurity in BDD and BNDD diamonds, the samples BDD-2 and BNDD-2 were tested by XPS. As shown in Fig. 3, beside the C 1s peak, both XPS spectra show obvious O 1s peak which may be the result of surface oxidation. The N 1s peak is very intensive in sample BNDD-2, nevertheless hardly observable in sample BDD-2. It shows a good evidence that nitrogen impurity has been incorporated into the boron-doped diamond lattice by the additive in the growth system. The N 1s peak of BDD-2 can be deconvoluted into two peaks with the binding energies of 399.3 eV and 400.0 eV, which are assigned to the sp^3 N–C bonding and the long N–C bond, respectively. And the N 1s peak of BNDD-2 can not be separated and present a strong peak at 399.3 eV assigned to sp^3 N–C bonding.[19–21]

We did not observed the peak relating to B–N bond in XPS result of co-doped diamond (BNDD-2). However, it can not be concluded that there is no B–N bond existing in such diamond, because the complicated circumstance of impurity in the co-doped diamond affects detecting significantly. Theoretical researches demonstrated that B–N dimer impurity in diamond has a negative formation energy of −0.17 eV.[22,23] It indicates that B–N dimer impurity is a very stable compound impurity and a potentially present cluster in multiple types of diamonds, especially in boron and nitrogen co-doped diamonds. We believe the bonding of B–N exists in such diamonds, despite the fact we did not detect them.

Raman spectroscopy is essential and familiar in boron-doped diamond research because it provides abundant information relevant to boron impurity and properties of diamonds. The Raman peak of diamond at 1332 cm^{-1} (the zone-center optical phonon line) shifts with the variation in property of diamonds, e.g., tensile stress in diamond leading to redshift of diamond Raman peak. The full width at half maximum (FWHM) of the diamond peak is also considered to be related to crystallinity (narrower FWHM corresponds to higher crystallinity).[24]

Samples were tested by Raman spectroscopy with an excitation source of 532 nm at room temperature. Raman spectra of the as-grown surfaces and interiors (polished surfaces) of four diamonds are shown in Figs. 4(a) and 4(b), no peaks due to amorphous carbon or graphite phase were detected. The diamond peak position (X_c) and FWHM of the Raman peaks of interiors of samples were compared and listed in the insert of Fig. 4(a). From the Raman results, it is found that the increase of boron additive in the growth system leads to redshift of X_c (from 1332.01 cm^{-1} to 1330.34 cm^{-1}) and broadening of FWHM (from 4.39 cm^{-1} to 6.36 cm^{-1}). In BNDD-1 and BNDD-2, the incorporation of nitrogen impurity leads to shift of X_c to the higher wavenumber (from 1330.34 cm^{-1} to 1331.00 cm^{-1}) and the narrowing of FWHM (from 6.36 cm^{-1} to 4.14 cm^{-1}). It seems that boron and nitrogen co-doped diamonds have better crystallization than boron doped diamonds.

Differing from other doping elements in diamonds, boron impurity allows some forbidden states to exist in Raman spectroscopy. As shown in Figs. 4(a) and 4(b), a series of additional bands at 580 cm^{-1}, 900 cm^{-1}, and 1042 cm^{-1} can be observed in the Raman spectra, which is related to the defect-induced activity of density of phonon states (DOS) of diamonds.[25] These bands are frequently observed in diamond with high boron concentration, barely found in low boron doped diamonds.[24–26] In Raman spectra of the as-grown surfaces shown in Fig. 4(b), spectra of BDD-1, BNDD1, and BNDD-2 present evident features of these bands (identical with features of interiors of diamonds). Such additional bands indicate that the samples have high boron concentration but still below the threshold of metal–insulator transition level.[6,7] The Raman spectrum of surface of sample BDD-2 shows distinct features of "500 cm^{-1} band" located at 470 cm^{-1}, the shift is due to the higher boron concentration in the diamond surface. The appearance of the 500 cm^{-1} band means that the concentration of boron reaches heavily doped level, and the band was attributed to boron dimer on diamond surface.[6,7] The difference between Raman spectra on surface and interior of BDD-2 comes from the difference of boron concentration. Boron impurity has an upper limit of solubility in diamond lattice, however is more likely to bond with carbon atoms (even form boron dimer) on the surface because of abundant vacancy on as-grown surface, so as to achieve higher boron concentration on surface of diamond.

The asymmetry of 1332 cm^{-1} diamond peak was frequently observed in highly and heavily boron doped diamonds, which is attributed to the Fano effect (a quantum interaction between discrete zone center Raman phonon and transitions from impurity band to continuum state composed of excited acceptor states and valence band) and is called Fano line shape.[27–30] Generally, the increasing boron concentration in diamond intensifies the Fano effect in Raman spectroscopy. As shown in Fig. 4(b), the asymmetry is very evident in spectra of the first three samples, comparatively weaker in spectra of BNDD-2. This indicates that the Fano effect was weakened by incorporation of nitrogen impurity in boron doped diamonds.

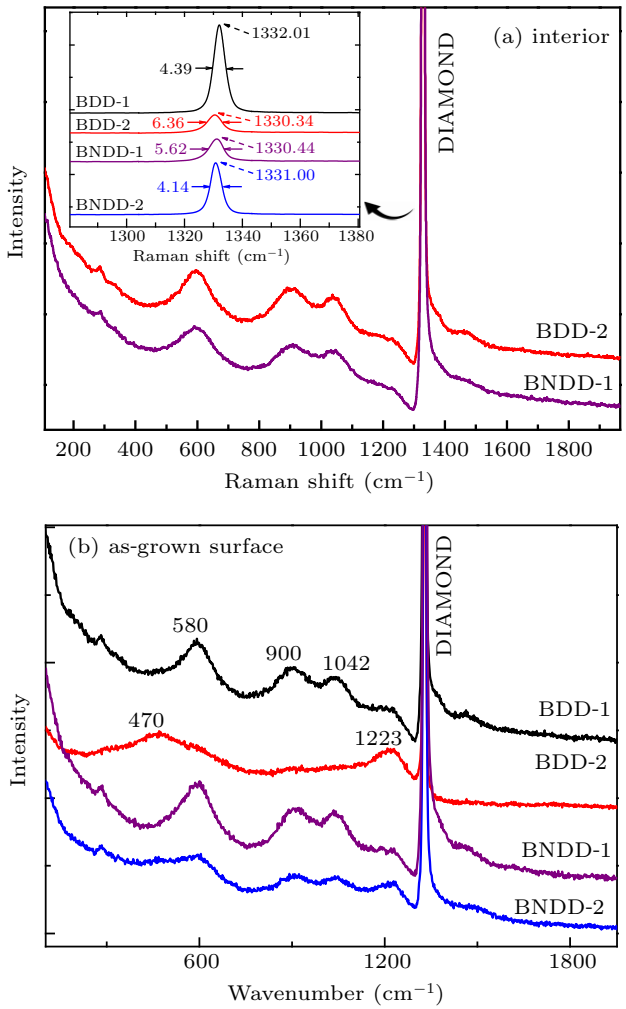


Fig. 4. (a) Raman spectra of interiors of samples BDD-2 and BNDD-1, the insert shows fitting curves of 1332 cm^{-1} peak of all four samples. (b) Raman spectra of as-grown surfaces of four samples. Peak "DIAMOND" is the diamond Raman peak (the zone-center optical phonon line) and the lines were moved vertically for clarity.

The infrared spectra of four polished diamond crystals are shown in Fig. 5. The band of 1290 cm^{-1} originates from the one-phonon-absorption of boron impurities in diamond, corresponding to the phonon energy of 160 meV. Peaks at 2460 cm^{-1}, 2800 cm^{-1}, and 2927 cm^{-1}, as shown in the spectrum of BNDD-2, correspond to transitions to the first, second, and third excited states of the bound hole, corresponding to activation energies of 304 meV, 347 meV, and 363 meV, respectively.[31–33] The infrared spectrum of BNDD-2 belongs to the typical infrared spectra of synthesized boron doped diamonds.[31,33] However, in the spectrum of BDD-1, the three peaks assigned to the transitions of bound hole are hardly observable because of photoionization continuum. The photoionization continuum, which generally starts at around 370 meV (activation energy of boron acceptor), is phonon-repeated and extends well into the visible. It is also responsible for the bluish color of type IIb diamonds.[1,31] As the increase of boron acceptor concentration in diamonds, the wave functions of adjacent B atoms overlap, the photoionization continuum intensifies and threshold shifts to the direction of low energy.[33,34]

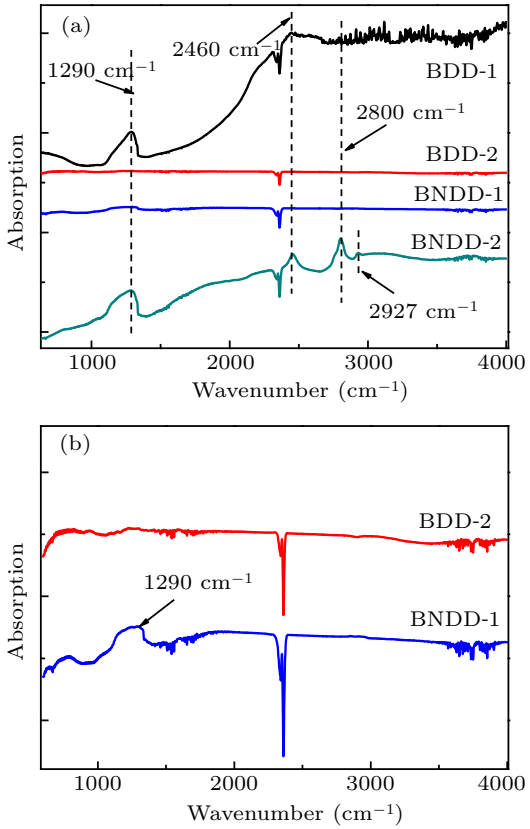


Fig. 5. FTIR absorption spectra of boron doped diamonds (BDD-1 and BDD-2) and boron/nitrogen co-doped diamonds (BNDD-1 and BNDD-2) (a) and the amplification of spectra of BDD-2 and BNDD-1 (b). The curves were moved vertically for clarity.

Therefore, the infrared spectra of BDD-2 and BNDD-1 with higher boron concentration are overwhelmed by photoionization continuum, no obvious B-related absorption peaks are found, typical highly B-doped diamond infrared spectra.[8] In addition, the 1290 cm^{-1} band and a slight declination of photoionization continuum at low energy region can be observed in the spectrum of BNDD-1. It indicates that the boron concentration in sample BNDD-1 slightly decreases as the incorporation of nitrogen. Thus, based on analysis above, the infrared spectra present a convincing semi-quantitative picture of the effects of the interaction of boron and nitrogen in

HPHT synthesized diamonds. We find that the concentration of boron acceptor in the diamond increases with the increasing boron additive content in the growth system, and decreases with the incorporation of nitrogen impurity. This is probably due to changes in the composition of the growth catalyst caused by nitrogen-containing additive affecting concentration of boron and nitrogen in the diamond lattice, and due to compensation of nitrogen donors for boron acceptors in the diamond lattice.

The Hall effect of samples was measured at room temperature by the four-probe method. The results are listed in Table 1. All samples exhibit p-type semiconducting properties, and the sample BDD-2 has the lowest resistivity of 0.9 Ω·cm and the highest carrier concentration of 7.4×10^{17} cm^{-3} at room temperature. The mobility of samples BDD-1 and BDD-2 is very low, because the mobility of samples BDD-1 and BDD-2 is mainly limited by the scattering caused by the neutral boron impurities. As the investigation of Hall hole mobility in boron-doped diamond by Pernot *et al.*,[9] in BDD semiconductors with high boron concentration (below the threshold of metal–insulator transition), electrical neutral boron impurities play a major role in carrier scattering, which is considered to be the main reason for limiting the conductivity of boron-doped diamonds with high boron concentration. The carrier concentration of BNDD-1 and BNDD-2 samples is much lower than that of the first two samples, which could be due to the increasing activation energy caused by the lower boron concentration and nitrogen compensating for the boron acceptor in the crystal. However, it is interesting to found that the mobility of BNDD-1 and BNDD-2 is much higher than that of BDD-1 and BDD-2. The highest mobility of sample BNDD-1 reached 980 $cm^2\cdot V^{-1}\cdot s^{-1}$. Two factors are considered to account for the increase in mobility of boron/nitrogen co-doped samples. (I) As the results of Raman spectroscopy, the samples of BNDD have better crystallinity than BDD, which benefits the carriers mobility in diamonds. (II) As the results of FTIR spectra, the incorporation of nitrogen obviously decreases the boron impurity concentration, especially dominant unionized neutral boron atoms, which is responsible for the low mobility in boron-doped diamonds.

Table 1. Conditions of additives in growth system and Hall measurement results. ρ is the resistivity; μ is the Hall mobility, and n is the density of free carriers.

Sample	Additive content in growth system (wt.%)			ρ (Ω·cm)	μ ($cm^2\cdot V^{-1}\cdot s^{-1}$)	n (cm^{-3})
	Boron	Ti	NaN_3			
BDD-1	2	5	0	2.28	2.5×10^1	1.09×10^{17}
BDD-2	4	5	0	0.9	0.9×10^1	7.4×10^{17}
BNDD-1	4	0	0.5	5.7	9.8×10^2	0.01×10^{17}
BNDD-2	4	0	1	9.5	3.2×10^2	0.02×10^{17}

4. Conclusions

In summary, boron doped diamonds and boron/nitrogen co-doped single-crystal diamonds with low electrical resistivity were synthesized by temperature gradient growth method under HPHT conditions. SEM, XPS, Raman and FTIR of boron doped and boron/nitrogen co-doped diamonds were analyzed. The results of FTIR spectroscopy present a semi-quantitative picture of the effects of the interaction of boron and nitrogen in HPHT synthesized diamonds. The results of Hall effect show that all samples present p-type conductivity. Boron and nitrogen co-doped diamonds present lower carrier concentration, but higher mobility than boron doped diamonds as incorporation of nitrogen. We consider that the increase in mobility may probably be attributed to the decreased neutral boron impurity level and the improvement of crystallinity. The results would be useful for further investigations about electrical properties of HPHT single crystal and co-doping of diamonds in the future.

References

[1] Thonke K 2003 *Semiconductor Science & Technology* **18** S20

[2] Isberg J, Hammersberg J, Johansson E, Wikstrom T, Twitchen D J, Whitehead A J, Coe S E and Scarsbrook G A 2002 *Science* **297** 1670

[3] Prikhodko D, Tarelkin S, Bormashov V, Golovanov A, Kuznetsov M, Teteruk D, Volkov A and Buga S 2016 *MRS Commun.* **6** 71

[4] Volpe P N, Pernot J, Muret P and Omnès F 2009 *Appl. Phys. Lett.* **94** 92

[5] Klein T, Achatz P, Kacmarcik J, Marcenat C, Gustafsson F, Marcus J, Bustarret E, Pernot J and Omnes F 2007 *Phys. Rev. B* **75** 165313

[6] Blank V, Buga S, Bormashov V, Denisov V, Kirichenko A, Kulbachinskii V, M Kuznetsov, Kytin V, Kytin G and Tarelkin S 2015 *Europhys. Lett.* **108** 67014

[7] Ekimov E A, Sidorov V A, Bauer E D, Mel'Nik N N, Curro N J, Thompson J D and Stishov S M 2004 *Cheminform.* **19** 351

[8] Locher R, Wagner J, Fuchs F, Wild C, Hiesinger P, Gonon P and Koidl P 1995 *Materials Science & Engineering B* **29** 211

[9] Pernot J, Volpe P N, Omnès F, Muret P, Mortet V and Haenen K 2010 *Phys. Rev. B* **81** 205203

[10] Liang Z Z, Kanda H, Jia X P, Ma H A, Zhu P W and Guan Q F 2006 *Carbon* **44** 913

[11] Lu Z Y, Wang Y K, Fang S, Cai Z H, Zhao Z D, Wang C X, Ma H A, Chen L C and Jia X P 2020 *Chin. Phys. B* **29** 128103

[12] Yiming Z, Larsson F and Larsson K 2013 *Theoretical Chemistry Accounts* **133** 1432

[13] Sonoda S, Won J H, Yagi H and Hatta A 1997 *Appl. Phys. Lett.* **70** 2574

[14] Hu M, Bi N, Li S, Su T, Hu Q, Ma H and Jia X P 2017 *CrystEngComm* **19** 4571

[15] Liang Q, Yan C S, Meng Y, Lai J, Krasnicki S, Mao H K and Hemley R J 2009 *J. Phys.: Condens. Matter* **21** 364215

[16] Lin IN, Hsu T, Lin G-M, Chou Y-P, Chen TT and Cheng H F 2003 *Journal of Vacuum Science & Technology B: Microelectronics and Nanometer Structures* **21** 1074

[17] Miao X, Chen L, Ma H, Fang C, Guo L, Fang S, Wang Y and Jia XP 2018 *CrystEngComm* **20** 7109

[18] Miao X, Chen L, Ma H, Fang C, Guo L, Wang Z and Jia X P 2019 *CrystEngComm* **21** 3961
[19] Fang C, Shen W, Zhang Y, Mu P, Zhang Z and Jia X P 2019 *Crystal Growth & Design* **19** 3955
[20] Titantah J T and Lamoen D 2007 *Diamond & Related Materials* **16** 581
[21] Sun S, Jia X, Zhang Z, Li Y, Yan B, Liu X, Ma HA and Jia XP 2013 *J. Crystal Growth* **377** 22
[22] Croot A, Othman, M Z, Conejeros S, Fox N A and Allan N L 2018 *J. Phys.: Condens. Matter* **30**
[23] Li R B 2005 *Solid State Commun.* **135** 155
[24] Mavrin B N, Denisov V N, Popova D M, Skryleva E A, Kuznetsov M S and Nosukhin S A 2008 *Phys. Lett. A* **372** 3914
[25] Blank V D, Denisov V N, Kirichenko A N, Kuznetsov M S, Mavrin B N and Nosukhin S A 2008 *Diamond & Related Materials* **17** 1840
[26] Karna S K, Martyshkin D V, Vohra Y K and Weir S T 2013 *MRS Proceedings* 1519 mrsf12-1519-mm03-27.
[27] Liu X, Chen X, Singh D J, Stern R A, Wu J, Petitgirard S, Bina C R and Jacobsen S D 2019 *Proc. Natl. Acad. Sci. USA* **16** 7703
[28] Pruvost F and Deneuville A 2001 *Diamond & Related Materials* **10** 531
[29] Mortet V, Vlčková Živcová Z, Taylor A, Frank O, Hubík P and Trémouilles D 2017 *Carbon* **115** 279
[30] Wang Y G, Lau S P, Tay B K and Zhang X H 2002 *J. Appl. Phys.* **92** 7253
[31] Mortet V, Pernot J, Jomard F, Soltani A, Remes Z and Barjon J 2015 *Diamond and Related Materials* **53** 29
[32] Smith S D and Taylor W 1962 *Proc. Phys. Soc.* **79** 1142
[33] Collins A T, Dean P J, Lightowlers E C and Sherman W F 1965 *Phys. Rev.* **140** 1272
[34] Locher R, Wagner J, Fuchs F, Maier M, Gonon P and Koidl P 1995 *Diamond & Related Materials* **4** 678